[PROC. OF JSCE Structural Eng./Earthquake Eng. Vol. 2, No. 2 October 1985]

AN EXPERIMENTAL STUDY ON ULTIMATE STRENGTH OF THIN-WALLED BOX STUB-COLUMNS WITH STIFFENERS SUBJECTED TO COMPRESSION AND BENDING

By Hiroshi NAKAI, Toshiyuki KITADA** and Toshihiro MIKI****

This paper presents the experimental study on the ultimate strength of thin-walled box stub-columns with the longitudinal stiffeners subjected to compression and bending. Eight columns were tested up to failure under the conditions of uniaxial and eccentrical compressions. These results were arranged from various point of views and the ultimate strength was plotted as the interaction curves of compression and bending. By introducing a plate slenderness for the stiffened box stub-columns, an empirical formula for evaluating their ultimate strength was proposed herein.

1. INTRODUCTION

In Japanese Specification for Highway Bridges[1] (JSHB) and other foreign specifications[2),3)], the plate elements with comparatively large plate slenderness can be utilized for designing the thin-walled box columns such as steel piers and pylons of cable-stayed or suspension bridges. It will not be able to evaluate exactly the ultimate strength of such structures without considering the local buckings of thin plates.

For the box stub-columns without stiffeners, the ultimate strength under the combined actions of compression and bending has already been investigated through the experimental and analytical studies and their interaction curves including the effects of local buckling were proposed by the authors[4),5)]. Then, it is possible to evaluate the accurate ultimate strength of thin-walled box column members by using these interaction curves[6)].

The ordinary columns such as used for the steel piers[7)] are, however, composed of the stiffened plates with many longitudinal stiffeners, thus it is also necessary to inquire the ultimate strength of box stub-columns built by the stiffened plates.

Although a lot of researches on the ultimate strength of isolated stiffened plates subjected to uniaxial compression can be found hitherto[8)~10)], one can scarcely find those of stub-columns composed of the stiffened plates, except the expermental studies by Fukumoto et al.[11),12)], which were conducted for seven stub-columns under uniaxial compression. Therefore, much more date should be needed to clarify the ultimate strength of stiffened box stub-column subjected to not only uniaxial compression but also bending.

* Member of JSCE, Dr. Eng., Professor, Dept. of Civil Eng., Osaka City University
** Member of JSCE, Dr. Eng., Associate Professor, Dept. of Civil Eng., Osaka City University
*** Member of JSCE, M. Eng., Research Associate, Dept. of Civil Eng., Osaka City University
(Sugimoto 3-3-138, Sumiyoshi-ku, Osaka 558)

This paper reports the experimental study on the thin-walled box stub-columns stiffened by the longitudinal stiffeners. Eight stub-columns were tested under the conditions of uniaxial and eccentrical compression. The collapse behaviors and ultimate strength were examined from various standpoints. Then, an empirical formula for evaluating the ultimate strength of stiffened stub-columns is proposed in the form of interaction curves by introducing a plate slenderness.

2. EXPERIMENTAL STUDY

(1) Design of Test Specimen

By referring the survey results of actual steel piers[7], nine test specimens were built up as shown in Fig. 1. In designing these specimens, the following points were taken into considerations ;

a) Dimensions

The cross-sectional dimensions of specimens were determined as the width of flange plate, $B=360$ mm, and that of web plate, $D=480$ mm, so as to conduct the failure tests within the limit of our loading devices (see Fig. 2). The length of specimen, l, was decided as the slenderness ratio $l/r \cong 10$ to avoid the column buckling of specimens, in which r is the radius of gyration.

b) Plate slendernesses of stiffened plates

The plate slendernesses R_f and R_w (their representative is designated by R) for stiffened flange and web plates are, respectively, defined by ;

$$R_f=\frac{B}{(n_f+1)\cdot t_f}\cdot\sqrt{\frac{12(1-\mu^2)}{k\pi^2}}\cdot\sqrt{\frac{\sigma_{fy}}{E}} \quad \cdots\cdots (1)$$

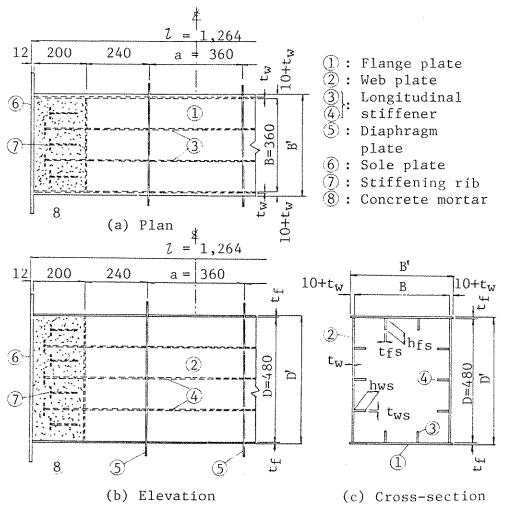

Fig. 1 Details of test columns (Dimension : mm).

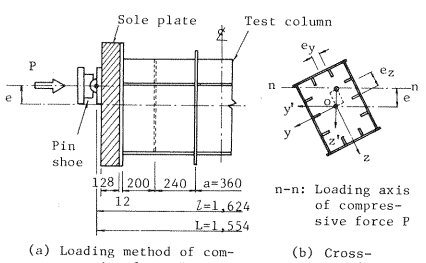

Fig. 2 Loading device (Dimension : mm).

$$R_w=\frac{D}{(n_w+1)\cdot t_w}\cdot\sqrt{\frac{12(1-\mu^2)}{k\pi^2}}\cdot\sqrt{\frac{\sigma_{wy}}{E}} \quad \cdots\cdots (2)$$

and set as $R_f \cong 0.4$ and 0.76, $R_w \cong 0.4$ and 0.76, where t_f, n_f : thickness and numbers of longitudinal stiffeners of flange plate, t_w, n_w : thickness and numbers of longitudinal stiffener of web plate, σ_{fy}, σ_{wy} : yield point of flange and web plate including their stiffeners, E : Young's modulus ($=2.06\times 10^5$MPa), μ : Poisson's ratio ($=0.3$), k : buckling coefficient ($=4.0$).

c) Longitudinal stiffeners

The spacing of longitudinal stiffeners was decided as 120 mm to correspond to the actual stiffened plates, and they were designed so as to coincide their relative flexural rigidities, γ, with the minimum values, γ_{req}, required by JSHB.

d) Diaphragms

The diaphragms were designed to form the stiffened plates with the aspect ratios $a/B=1.0$ and $a/D=0.75$. The rigidities of diaphragms were taken as 3~5 times of the required rigidity specified by JSHB to make the nodes of buckling waves at these locations. These diaphragms were, then, fabricated as the open ring frame by four strip plates with 50 mm $\times$ 4.5 mm.

e) Used steel and welding condition

The mild steels with the thicknesses 3.2 and 6 mm, made of grade SS41, were used as the material of flange, web plates and longitudinal stiffeners. Thus, the size of welding was decided as 3～4 mm since the steel plates were comparatively thin. Only the diaphragms were welded discontinuously.

f) Reinforcement at ends of specimens

In order to avoid the local buckling and to ensure the uniform distributions of applied compressive load at both the ends of specimens, the stiffening ribs with Tee cross-section were attached and then the cement mortar was poured into the end parts of specimens (see Fig. 1).

(2) Cross-sectional Dimension and Corresponding Parameter

The cross-sectional dimensions and the corresponding parameters of test specimens can be summarized in Tables 1 and 2. The specimens S1～S4 were tested under the uniaxial compression. The plate slendernesses of stiffened plates, R_f and R_w, were changed into various combinations to clarify their influences on the ultimate strength of box stub-columns. While, the tests were carried out for the specimens S5～S8 under the conditions of eccentrical compression to inquire the ultimate strength of box stub-columns subjected to compression and bending simultaneously by setting $R_f=R_w\cong 0.4$ and $R_f=R_w\cong 0.76$. The remaining specimen S9 is the one for investigating the residual stresses, and the dimensions were identical to those of S4 and S6～S8.

(3) Loading Condition

The axial compressive loads, P, for test specimens S1～S8 were decided as follows.

Firstly, the maximum compressive stress, σ_c, of a box stub-colum subjected to the compressive force P and both the bending moments M_y and M_z with respect to the centroidal axes (y,z) will be given by ;

$$\sigma_c=P/A+M_y/W_y+M_z/W_z \cdots (3)$$

where W_y, W_z : section modulus with respect to axes (y,z), A : cross-sectional area of box stub-column.

If the load P is applied to a column with the eccentricities e_z and e_y from the axes (y,z) as shown in Fig. 2, the induced bending moments M_y and M_z will reduce to ;

$$M_y=P\cdot e_z,\quad M_z=P\cdot e_y \cdots\cdots (4)_{a,b}$$

Therefore, the eccentricities were regarded as $e_y=e_z=0$ for the specimens S1～S4. For the specimens S5, S6 and S7, the tests were performed by taking e_z and e_y so as to correspond to $P/A=M_y/W_y$ and $P/A=M_z/W_z$, respectively. Furthermore, the compressive force P was applied to the test specimen S8 with the eccentricities in both the axes y and z to fulfill a condition where $P/A=M_y/W_y=M_z/W_z$.

These loading conditions are listed in Table 3, in which the loading parameter, β, is defined as the ratio of bending moment $M_{y'}(=P\cdot e)$ around y'-axis (see Fig. 2) to axial force, which represents ;

$$\beta=(M_{y'}/M_{py})/(P/P_Y) \cdots\cdots (5)$$

Table 1 Dimensions, cross-sectional properties and slenderness parameters of test columns (SS41).

Items / Test columns	Dimensions and cross-sectional properties							Slenderness parameters		
	B' (mm)	D (mm)	t_f (mm)	t_w (mm)	2A (mm²)	r_y (mm)	r_z (mm)	R_f	R_w	R_{fw}
S1	392	481	5.85	5.92	12,345	188	152	0.407	0.402	0.404
S2	392	480	3.15	5.93	9,675	171	162	0.766	0.402	0.508
S3	387	480	5.93	3.18	8,900	205	140	0.402	0.758	0.545
S4	386	480	3.16	3.16	6,238	188	152	0.763	0.763	0.763
S5	392	480	5.88	5.92	12,313	183	152	0.405	0.402	0.403
S6	386	480	3.13	3.17	6,200	188	152	0.770	0.761	0.765
S7	386	480	3.20	3.15	6,264	188	152	0.754	0.766	0.761
S8	386	480	3.15	3.16	6,245	189	152	0.766	0.763	0.764
S9	386	480	3.15	3.16	6,245	188	152	0.766	0.763	0.764

Notes; A: Cross sectional area of box section.
ry and rz: Radius of gyration about y and z axis, respectively.
R_f: Eq.(1), R_w: Eq.(2), R_{fw}: Eq.(9)

Table 2 Dimension and cross-sectional properties of longitudinal stiffeners in test columns (SS41).

Items / Test columns	Flange plate					Web plate				
	h_{fs} (mm)	t_{fs} (mm)	δ_f	γ_f	γ_f/γ_{req}	h_{ws} (mm)	t_{ws} (mm)	δ_w	γ_w	γ_w/γ_{req}
S1	34.3	5.87	0.0956	12.0	1.422	34.4	5.89	0.0713	8.9	1.350
S2	24.7	3.10	0.0675	15.1	1.170	34.3	5.86	0.0707	8.6	1.310
S3	34.2	5.87	0.0941	11.4	1.394	24.7	3.16	0.0512	11.2	1.105
S4	25.3	3.16	0.0701	16.2	1.225	24.9	3.16	0.0528	12.4	1.225
S5	34.6	5.90	0.0964	12.2	1.465	34.2	5.86	0.0856	8.6	1.307
S6	24.8	3.13	0.0690	15.8	1.225	24.8	3.14	0.0513	11.5	1.137
S7	24.4	3.15	0.0667	14.1	1.088	24.4	3.15	0.0508	11.1	1.096
S8	24.6	3.14	0.0681	15.1	1.168	25.1	3.16	0.0524	12.1	1.197
S9	24.6	3.14	0.0681	15.1	1.168	25.1	3.16	0.0524	12.1	1.197

Notes; δ_f, δ_w : $\delta_f=h_{fs}t_{fs}/B/t_{fs}$, $\delta_w=h_{ws}t_{ws}/D/t_{ws}$.
γ : Relative flexural rigidity of longitudinal stiffener.
γ_f, γ_w : $\gamma_f=EI_{fs}/B/K_f$ for flange plate, $\gamma_w=EI_{ws}/D/K_w$ for web plate.
I_{fs}, I_{ws}: $I_{fs}=h_{fs}{}^3t_{fs}/3$, $I_{ws}=h_{ws}{}^3t_{ws}/3$
K_f, K_w: $K_f=Et_f{}^3/12/(1-\mu^2)$, $K_w=Et_w{}^3/12/(1-\mu^2)$
γ_{req} : Required minimum value of γ by JSHB.

Table 3 Loading conditions of test columns.

Items / Test columns	Eccentricity of compression load e_z (mm)	e_y (mm)	e (mm)	Loading parameters β
S1 S4	0.0	0.0	0.0	0.0
S5	14.32	0.0	14.32	0.847
S6	14.40	0.0	14.40	0.851
S7	0.0	12.60	12.60	0.891
S8	14.53	12.69	19.29	1.308

Notes; e_z, e_y and e: See Fig.2.
β: Eq.(5).

Table 4 Average mechanical properties of test columns (SS41).

Young's modulus E(MPa)	Poisson's ratio μ	Lower yield point σ_Y(MPa) t=3.2mm	t=6.0mm
2.1×10^5	0.3	302	295

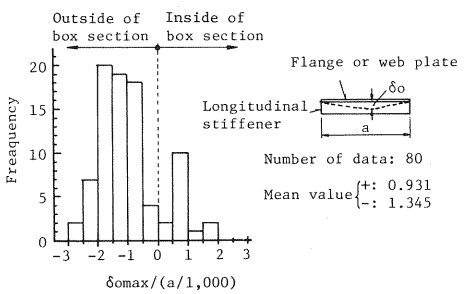

Fig. 3 Histogram of maximum initial deflections $\delta_{0\,max}$ at location of longitudinal stiffeners.

where $M_{py'}$: fully plastic moment of box stub-column with respect to y'-axis, and P_Y : fully plastic axial force, which can be estimated from ;

$$P_Y=2\cdot(A_f\cdot\sigma_{fy}+A_w\cdot\sigma_{wy}) \quad \cdots\cdots (6)$$

in which

$$\left.\begin{aligned} A_f&=B\cdot t_f+n_f\cdot h_{fs}\cdot t_{fs}\\ A_w&=D\cdot t_w+n_w\cdot h_{ws}\cdot t_{ws}\end{aligned}\right\} \quad \cdots\cdots (7)_{a,b}$$

(4) Loading Device

The compressive force was applied to the test specimens by using the special buckling devices with the capacity 5.88 MN[13] as shown in Fig. 2. The sole plates with thickness 128 mm were bolted to hold the flatness of both the ends of specimens, then the shoes were set with the eccentricity, e, from the centroid (see Table 3).

Through conducting the preliminary tests within the elastic ranges, these devices were adjusted several times until the strain distributions in the specimens were coincided with the theoretical ones, thereafter the load was gradually increased up to the failure.

3. MECHANICAL PROPERTY AND INITIAL IMPERFECTION OF TEST SPECIMEN

(1) Mechanical Property

The test specimens were assembled by nine steel plates (SS41), so that the tensile tests were carried out by 23 coupons (JIS No. 5). The average mechanical properties are summarized in Table 4.

(2) Initial Deflection

According to Ref. 14), it is obvious that the initial deflections, δ_0, at the position of longitudinal stiffeners significantly affect upon the ultimate strength of stiffened plates, since they behave as a column of Tee section including the effective width of plate panel and longitudinal stiffener. Therefore, δ_0 were measured at every one-eighth points of flange and web plates. The maximum initial deflections, $\delta_{0\,max}$, can be plotted in the form of a histogram as shown in Fig. 3.

From this figure, $\delta_{0\,max}$ falls within $\pm 3a/1\,000$ and 60% of them are greater than the tolerance, $a/1\,000$, for compressive columns provided by JSHB. The results of modal analysis according to Ref. 14) show that almost all the stiffened plates have the initial deflections of a sinusoidal mode with half wave and deform towards outside of box section.

(3) Residual Stress

The residual stresses were also measured by specimen S9, because the welding beads are somewhat large in comparison with the thickness of steel plates. The strain gages were used and measured after cutting the specimen by sawing machine with the width 20~30 mm.

Fig. 4 shows the residual stress distributions by modifying the measured results.

It is observed from this figure that the residual tensile stress, σ_{rt}, nearly is equal to yield stress, σ_y, at the junctions of longitudinal stiffeners and

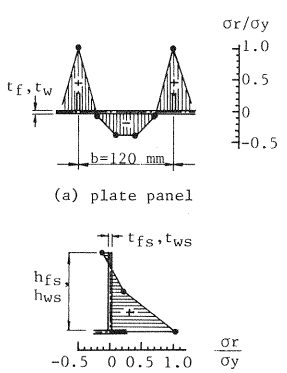

Fig. 4 Average residual stress distributions in test columns S 9.

the residual compressive stress, σ_{rc}, of middle part of plate panel is approximately $0.4\sigma_y$. Besides, the residual stress distributions in the longitudinal stiffeners vary linearly from σ_y until $\sigma_{rc}=0\sim0.25\ \sigma_y$ at their free edges.

4. TEST RESULT

(1) Failure Mode of Test Column

The failure modes at the central cross-sections of the specimens S 1～S 4 and S 5～S 8 are respectively shown in Figs. 5 and 6, from which the following points can be pointed out.

a) Specimens S 1～S 4 (Uniaxial compression)

It is clear from Fig. 5 that both the flange and web plates of specimens S 1 ($R_f=R_w\cong0.4$) and S 4 ($R_f=R_w\cong0.76$), which have almost the same plate slenderness R_f and R_w, deform towards outside of box section at the ultimate state. Whereas, the slender stiffened plates deform towards outside and the stocky ones deform towards inside of the box section in case where the specimens have the different plate slendernesses such as S 2 ($R_f\cong0.76$, $R_w\cong0.4$) and S 3 ($R_f\cong0.4$, $R_w\cong0.76$). In the former, it seems that the initial deflection modes towards outside of the box section may significantly affect upon the failure modes. In the latter, it is thought that the slender stiffened plates ($R\cong0.76$) bow towards outside of the box section at first and then the stocky ones ($R\cong0.4$) were pulled towards inside of the section to keep the right angle at the corners of box section.

b) Specimens S 5～S 8 (Eccentrical compression)

All the stiffened plates in a portion, where the compressive force is predominant, deform towards outside of box section as is seen from Fig. 6. This is caused by the initial deflection modes similar to the above ($\beta=0$).

Through the test specimens S 1～S 8, it is concluded that the all stiffened plates collapse in the form of buckling modes with a half wave in the longitudinal and transverse directions (thereafter referred to as the overall buckling of stiffened plate). Moreover, the buckling of plate panel between the longitudinal stiffeners (therafter referred to as the local buckling of stiffened plate) is observed in a corner part of box section of specimen S 8, since there occurs the remarkable compressive stresses due to biaxially eccentric loading (see Photo. 1).

(2) Load-Deflection Curve

The relationships between applied compressive force, P, and out-of-plane displacements of stiffened plates, δ, can be illustrated in Figs. 7 and 8, where P is non-dimensionalized by the following initial yield load P_y.

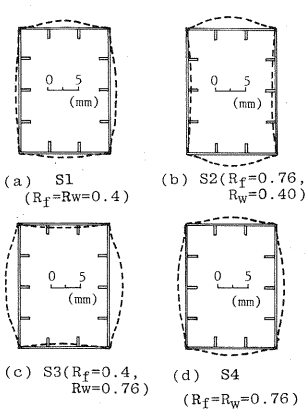

Fig. 5 Failure modes of test columns S 1～S 4 subjected to pure compression ($\beta=0$).

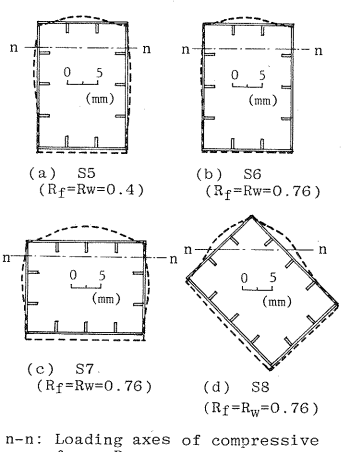

Fig. 6 Failure modes of test columns S 5～S 8 subjected to eccentrical compression.

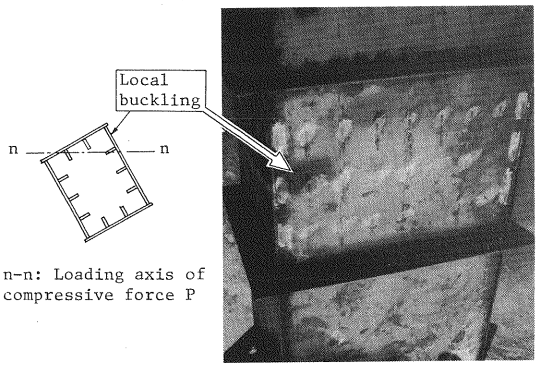

Photo 1 Local buckling of test colmn S 8.

$$P_y=\sigma_y/\{1/A+e_y/W_y+e_z/W_z\} \quad \cdots\cdots\cdots\cdots (8)$$

Noted that $e_y=0$ and $e_z=0$ for $\beta=0$, then P_y reduces to the axial squash load, P_y, in Eq. (6).

a) Specimens S3 and S4 (Uniaxial compression)

P-δ curves in Fig. 7 (a) for the stiffened plates in the specimen S3 ($R_f\cong 0.4$ and $R_w\cong 0.76$) show that δ of the slender web plate increases similarly in accordance with the load increment, but δ of the stocky flange plate increases suddenly directly before the ultimate load and behaves as the bifurcated buckling. On the other hand, it is obvious from Fig. 7 (b) that the deflections, δ, of all the stiffened plates increase at $P/P_y\cong 0.4$ in the specimen S4 ($R_f=R_w\cong 0.76$). These become larger at $P/P_y\cong 0.7$ and then this column results in failure at $P/P_y\cong 0.8$.

b) Specimens S6 and S8 (Eccentrical compression)

In the specimen S6, P-δ curve of a flange plate suejected to larger compression begins to bow monotonously at $P/P_y\cong 0.6$ and this column collapses at $P/P_y\cong 1.1$ as is seen from Fig. 8 (a). A fact $P_u>P_y$ indicates the significant stress redistributions from the flange plate to web plate, in spite of larger plate slenderness, $R\cong 0.76$, of this specimen.

The result of specimen S8 in Fig. 8 (b) shows that δ increases near $P/P_y\cong 0.85$, thus this specimen collapses at $P/P_y\cong 1.25$. The redundancy of post-yield strength is about 25% due to the trapezoidal compressive stress distributions of two adjacent stiffened plates in spite of the slender box stub-column ($R\cong 0.76$).

(3) Load-Strain Curve

Two distinct buckling loads, P_a/P_y and P_b/P_y, indicated in Fig. 9, are introduced by arranging the load-strain curve of the mid-section of specimens. The former corresponds to the overall buckling load of stiffened plates due to the initiation of flexural strain i. e., the difference between ε_{si} and ε_{so} are caused by the deflection of flange or web plates at the longitudinal stiffeners. The latter is the local buckling strength of plate panel between the longitudinal stiffeners, where the flexural strains ε_{pi} and ε_{po} have a discrepancy due to the deflection of plate panels.

These results can be summarized and

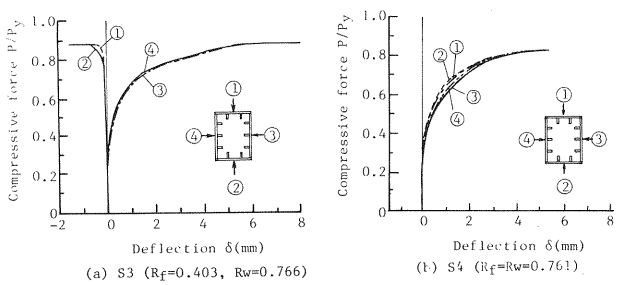

Fig. 7 P-δ curves of stiffened plates in test columns S 3 and S 4.

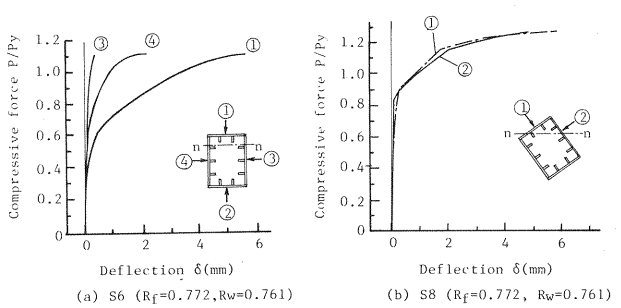

Fig. 8 P-δ curves of stiffened plates in test columns S 6 and S 8.

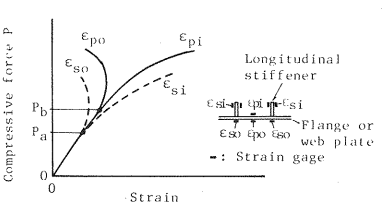

Fig. 9 Definition of buckling loads P_a and P_b of stiffened plates.

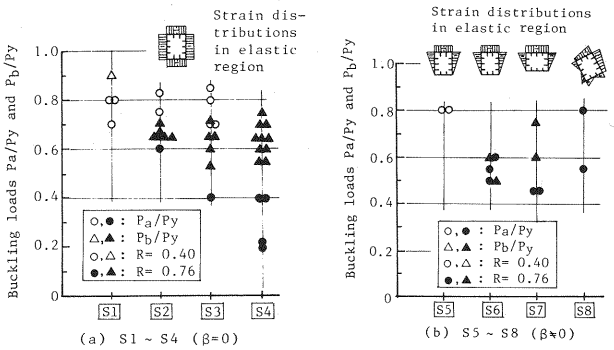

Fig. 10 Variations of buckling loads P_a/P_y and P_b/P_y in test columns.

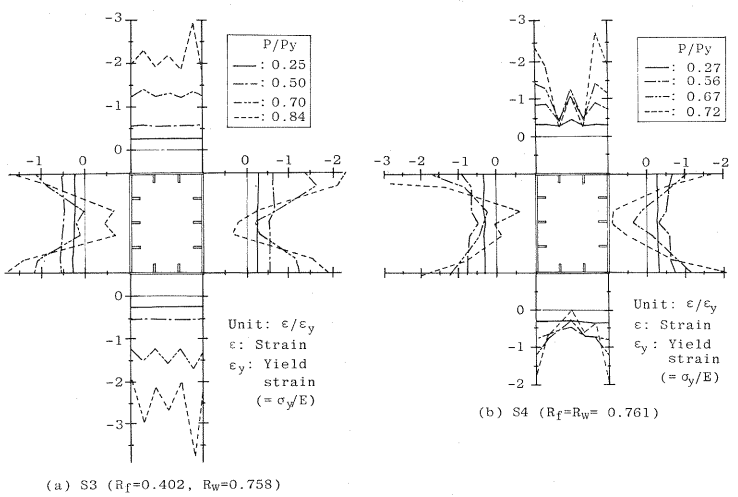

Fig. 11 Strain distributions at central cross-sections of test columns S 3 and S 4 subjected to pure compression.

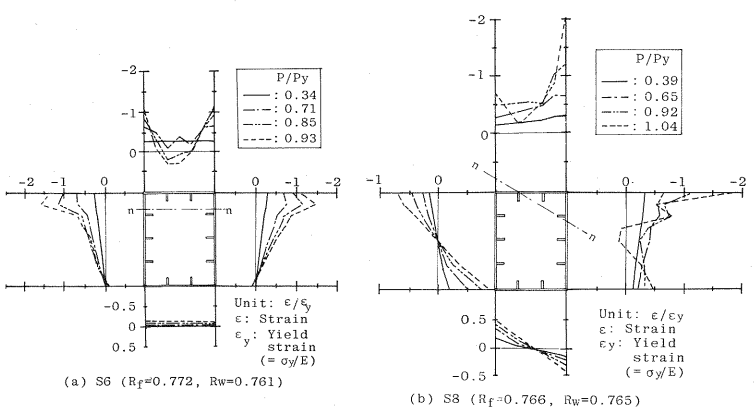

n-n : Loading axis of compressive force P

Fig. 12 Strain distributions at central cross-sections of test columns S 6 and S 8 subjected to eccentrical compression.

plotted corresponding to their plate slenderness as shown in Fig. 10.

It is observed from this figure that the stocky stiffened plates ($R \cong 0.4$) collapse mainly by the overall buckling of stiffened plates, whereas the slender ones ($R \cong 0.76$) have the tendency to collapse by the coupled buckling of overall buckling in the early loading stage and the succeeding local buckling. Especially, this tendency is predominant in the specimen S 4.

In the specimens S 2 and S 3 having the different plate slendernesses, the redundancy of ultimate strengths after the overall buckling of slender stiffened plates ($R \cong 0.76$) are, respectively, about 22% and 25%. Thus, the ultimate strengths of stub-columns seem to be heightened by the stocky stiffened plates.

(4) Strain Distribution

The variations of strain distributions in accordance with the load increment at the central cross-section of specimens are plotted in Figs. 11 and 12.

a) Specimens S 3 and S 4 (Uniaxial compression)

The overall buckling of stiffened web plates ($R_w \cong 0.76$) is already observed at $P/P_y \cong 0.70$ in specimen S 3 (Fig. 11 (a)) and their strain distributions are in greatly disorder. However, the strain distribution in the flange plates ($R_f \cong 0.4$) are comparatively uniform. In the specimen S 4 ($R_f = R_w \cong 0.76$), the strain distributions of all stiffened plates are also in disorder for each lower loading stages and result in failure (Fig. 11 (b)).

b) Specimens S 6 and S 8 (Eccentrical compression)

In the specimen S 6 (Fig. 12 (a)), the collapse is caused by the overall buckling of flange plate in a

compression side and the local buckling of the adjacent web plates, then the linear strain distribution is observed up to failure except the buckled portions. Although the specimen S8 (Fig. 12 (b)) is buckled locally at a corner part of compression at $P/P_y \cong 0.92$, the flange and web plates collapse by the overall buckling at the ultimate state.

5. ULTIMATE STRENGTH OF STIFFENED BOX STUB-COLUMN

The ultimate strength can be represented by axial compressive force P_u and bending moment $M_{uy}(=P_u \cdot e)$. Table 5 shows these values non-dimensionalized by P_Y and M_p.

(1) Ultimate Strength for Uniaxial Compression ($\beta=0$)

Let us now consider the variations of ultimate strength of specimens S1~S4 subjected to uniaxial compression.

According to Eqs. (1) and (2), the ultimate strength of stub-column is governed by two parameters R_f and R_w. Then, P_u/P_Y can be discussed by adopting the following new plate slenderness R_{fw} ;

$$R_{fw}=2\cdot(R_f\cdot A_f\cdot\sigma_{fy}+R_w\cdot A_w\cdot\sigma_{fw})/P_Y \quad \cdots\cdots (9)$$

This parameter is derived by the two assumptions that ; (i) ultimate strength of isolated stiffened plate subjected to uniaxial compression is represented by the linear function of plate slenerness $R(R_f$ or $R_w)$, (ii) ultimate strength of box stub-column is given by the sum of each stiffened plates. Thus derived R_{fw} also coincides with the plate slenderness of box stub-column by Fukumoto et al. [11)~12)]

The relationships between R_{fw} and P_u/P_Y can be plotted in Fig. 13, where the test results (seven box stub-columns composed of the stiffened plates with one or three longitudinal stiffeners) conducted by Fukumoto et al. are plotted and their empirical line is also drawn.

It can be seen from this figure that the relationships between P_u/P_Y and R_{fw} are linear and R_{fw} is the appropriate parameter for predicting the ultimate strength of box stub-columns within the region where $0.4 \leq R_{fw} \leq 0.8$. The results can also be represented by the least sqare method on the basis of an assumption that P_u/P_Y is a linear function of R_{fw} ;

$$P_u/P_Y=1.14-0.454\cdot R_{fw} \quad \cdots\cdots (10)$$

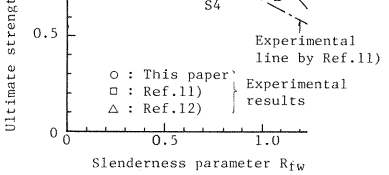

Fig. 13 Test results of ultimate strength P_u/P_Y of test columns subjected to pure compression.

Eq. (10) gives about 10% lower value than the empirical line proposed by Fukumoto et al., but the variation of P_u/P_Y due to R_{fw} has the similar tendency.

(2) Interaction Curve for Ultimate Compressive Force and Bending Moment

The relationships between P_u/P_Y and $(M_u/M_p)_{y'}$ can be plotted on the basis of results of specimens S1, S4 and S5~S8 having the almost same plate slenderness R_{fw} as shown in Fig. 14. In this figure, the interaction curves[5)] of box stub-columns subjected to compression and bending, i.e. ;

Table 5 Test results of ultimate strength P_u/P_Y and $(M_u/M_p)_{y'}$.

Items / Test columns	Slenderness parameters R_{fw}	Squash load P_Y (MN)	Fully plastic moment Mp(MNm)	Experimental results Pu (MN)	Mu (MNm)	(1) $\frac{Pu}{P_Y}$	(2) $\left(\frac{Mu}{Mp}\right)_{y'}$	(3) $l_u=\sqrt{(1)^2+(2)^2}$	Eq.(12) (4) l_u^*	Errors $\frac{(3)-(4)}{(3)}$ (%)
S1	0.404	3.645	-	3.600	0	0.988	0	-	-	-
S2	0.508	2.877	-	2.615	0	0.909	0	-	-	-
S3	0.545	2.653	-	2.330	0	0.878	0	-	-	-
S4	0.763	1.892	-	1.515	0	0.801	0	-	-	-
S5	0.403	3.636	0.615	2.284	0.327	0.628	0.532	0.823	0.814	1.1
S6	0.765	1.883	0.319	1.049	0.151	0.557	0.474	0.731	0.659	9.8
S7	0.761	1.895	0.267	0.905	0.114	0.478	0.426	0.640	0.618	3.4
S8	0.764	1.889	0.279	0.780	0.150	0.413	0.540	0.680	0.713	-4.9

Note; Mpy' : Fully-plastic moment about y'-y' axis (see Fig.14).

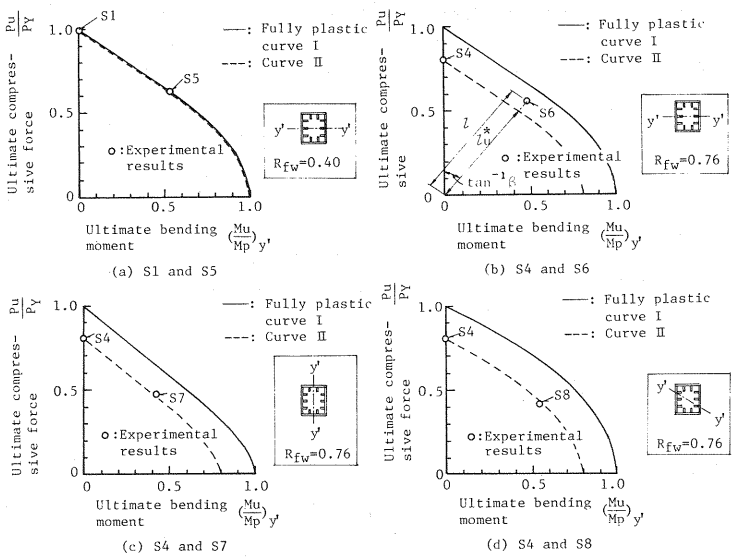

Fig. 14 Relationships between ultimate compressive strength P_u/P_Y and ultimate bending moment M_u/M_p of test columns.

Curve I : $(M_u/M_p)_{y'}=F(P_u/P_Y)$ ..... (11)

Curve II : $(M_u/M_p)_{y'}=k_{pl}\cdot F\cdot\{(P_u/P_Y)/k_{pl}\}$ ..... (12)

are drawn by solid and broken lines, respectively.

The curve I shows the fully plastic interaction curve, and the curve II is the contracted one of curve I on the scale k_{pl} which represents the non-dimensionalized ultimate strength of box stub-columns subjected to uniaxial compression. For the value of k_{pl}, the ultimate strengths of specimens S 1 and S 4 are used as the reference values.

In addition to the above, the perpendicular distance between origin (0, 0) and $\{(P_u/P_Y), (M_u/M_p)_{y'}\}$ is denoted by l_u for the test results and l_u^* for the calculated ones from Eq. (12) under the given load parameter β. These results are also summarized in Table 5.

It is observed from Fig. 14 (a) that the test results of specimens S 1 and S 5 ($R_{fw}\cong 0.4$) coincide with the curve I, thus these specimens collapse at the fully plastic state. While, the test results of specimens S 4 and S 6～S 8 ($R_{fw}\cong 0.76$), plotted in Figs. 14 (b)～(d), show that they lay within curve I and fail prior to the fully plastic state.

The difference between l_u and l_u^* falls within the range -5 to 10% for the specimens S 5 through S 8 and almost all the test results are close to curve II. This fact suggests that the ultimate strength of box stub-column decreases with a constant ratio from the fully plastic curve I and almost is equal to curve II on the analogy to those of unstiffened box stub-columns under compression and bending[5].

6. DISCUSSION FOR ULTIMATE STRENGTH OF STIFFENED BOX STUB-COLUMN SUBJECTED TO COMPRESSION AND BENDING

The interaction curve of ultimate strength for a stiffened box stub-column can be evaluated by combining the above results as follows ;

(1) the plate slenderness R_{fw} is firstly determined by Eq. (9),

(2) the corresponding ultimate strength $P_u/P_Y=k_{pl}$ is then found through the substitution of R_{fw} into Eq. (10) and

(3) the substitution of k_{pl} into Eq. (12) leads to the ultimate interaction curve for ultimate strength, provided that the conditions where $0\leq\beta\leq 1.0$, $0.4\leq R_{fw}\leq 0.8$ and $\gamma\geq\gamma_{req}$.

Although there are a few remaining problems to be solved for $\beta>1$, i.e., for the case where the bending moment is predominant rather than the axial force, the ultimate interaction curves mentioned in the above can be applied to the ultimate strength analysis of stiffened box columns under combined local and overall buckling. Thus, this paper can offer a valuable information concerning the rational design of thin-walled box column members.

7. CONCLUSION

In this paper, the collapse behaviors and ultimate strength of stiffened box stub-columns were reported by conducting the experimental study on eight test specimens subjected to uniaxial or eccentrical compression, then an empirical formula of the interaction curve for evaluating the ultimate strength was proposed. The main conclusions obtained in this paper can be summarized as follows ;

(1) In a case of the stub-columns with the different plate slendernesses R_f and R_w under uniaxial compression, their redundant strength up to failure becomes large after the overall buckling of the slender stiffened plates.

(2) In a case of eccentrical compression, the redundant strength after initial yield until ultimate state is also large.

(3) The relationships between ultimate strength and plater slenerness R_{fw} in the stub-columns subjected to uniaxial compression are represented by a linear line, then an empiuical ultimate strength can be proposed by using R_{fw}.

(4) Based upon the interaction curve of ultimate strength of box stub-columns subjected to compression and bending, almost all the test results are laid on curve Ⅱ derived by multiplying the non-dimensionalized ultimate strength of stub-column subjected to uniaxial compression, k_{pl}, to the fully plastic curve Ⅰ.

(5) An empirical formula for setting the ultimate interaction curve of stiffened box stub-columns subjected to combined actions of compression and bending can be proposed under the conditions where $0\leq\beta\leq1.0$, $0.4\leq R_{fw}\leq0.8$ and $\gamma\geq\gamma_{erq}$ according to JSHB.

8. ACKNOWLEDGMENTS

This study was sponsored by Hanshin Highway Public Corporation. In conducting the experimental study, the authors would like to appreciate the energetic supports by Mr. M. Sakano, post graduate student of Osaka City University.

REFERENCES

1) Japanese Road Association : Specifications for Highway Bridges, Feb. 1980.
2) British Standards Institution : BS 5400, Steel concrete and composite bridges, Part 3 Gode of practice for design of steel bridges, April 1982.
3) Deutscher Ausschuβ für Stahlbau : DASt Ri-012, Beulsicherheitsnachweise für Platten, Okt. 1978.
4) Nakai, H., Kitada, H., and Miki, T. : Ultimate Stregth of Thin-Walled Box Stub-Columns, Proc. of JSCE, Struct. Eng./Earthq. Eng., Vol. 2, No. 1 pp. 25~34, April 1985.
5) Nakai, H., Kitada, T. and Miki, T. : Interaction Curve of Thin-Walled Box Stub-Column subjected to Compression and Bending for applying to Overall Buckling Analysis of Columns, Proc. of JSCE, Struct. Eng./Earthq. Eng., Vol. 2, No. 2, Oct. 1985.
6) Nakai, H., Emi, S. and Miki, T. : A Study on In-Plane Buckling Collapses of Thin-Walled Steel Frames subjected to Vertical Loads, The 31st Structural Engineering Symposium of JSCE, pp. 79~92, April 1985.
7) Nakai, H., Kawai, A., Yoshikawa, O., Kitada, T. and Miki, T. : A Survey on Steel Piers, Bridge and Foundation Engineering, Vol. 16, No. 6, pp. 35~40, No. 7, pp. 43~49, 1982.
8) Komatsu, S. and Kitada, T. : An Experimental Study on the Ultimate Strength of Stiffened plates, Proc. of JSCE, No. 255, pp. 47~61, Nov. 1976.
9) Kanai, M. : A Study on the Safety of Box Girder Bridges, Technical Memorandum of Public Works Research, No. 1436, Bridge Division Public Works Research Institute, Ministry of Construction, Dec. 1978.
10) Komatsu, S. and Kitada, T. : Practical Method of Calculation for the Ultimate Strength of Stiffened Plates under Compression,

Proc. of JSCE, No. 302, pp. 1～13, Oct. 1980.

11) Usami, T. and Fukumoto, Y. : Local and Overall Buckling Tests of Compression Members and an Analysis based on the Effective Width Concept, Proc. of JSCE, No. 326, pp. 41～50, Oct. 1982.

12) Usami, T., Fukumoto, Y. Aoki, T. and Matsukawa, A. : Experimental Study on Eccentrically Loaded Stiffened Box Columns, No. 350／I-2, pp. 197～205, Oct. 1984.

13) Nakai, H., Kitada, T. and Miki, T. : A Compression Testing Machine with Capacity 600 tons for Experimental Researches on Large-Sized Members in Bridge Structures, Memoirs of the Faculty of Engineering, Osaka City University, Vol. 23, pp. 205～218, Dec. 1982.

14) Komatsu, S. : Statistical Study on the Inital Deformations and the Ultimate Strength of Steel Bridge Members, Journal of JSSC, Vol. 16, No. 179, pp. 10～43, 1980.

(Received March 4 1985)